

Multilayered Semiconductor (CdS/CdSe/ZnS)-Sensitized TiO₂ Mesoporous Solar Cells: All Prepared by Successive Ionic Layer Adsorption and Reaction Processes

Hyo Joong Lee,^{*,†} Jiwon Bang,[‡] Juwon Park,[‡] Sungjee Kim,[‡] and Su-Moon Park^{*,†}

[†]Interdisciplinary School of Green Energy, Ulsan National Institute of Science and Technology (UNIST), Ulsan, 689-805, Korea (ROK), and [‡]Department of Chemistry, Pohang University of Science and Technology (POSTECH), Pohang, 790-784, Korea (ROK)

Received July 20, 2010. Revised Manuscript Received August 24, 2010

A model semiconductor-sensitizer layer of CdSe with under- or overlayers of CdS or ZnS by pre- or postadsorption was prepared on the surface of mesoporous TiO₂ films by a series of successive ionic layer adsorption and reaction (SILAR) processes in solutions containing corresponding cations and anions. The growth of each semiconductor layer was monitored by taking UV-visible absorption spectra and high-resolution transmission electron microscopy (TEM) images. The all SILAR-prepared multicomponent sensitizer consisting of CdS/CdSe/ZnS layers was evaluated in a polysulfide electrolyte solution as a redox mediator in regenerative photoelectrochemical cells. The CdS and ZnS layers with the CdSe layer sandwiched in between were found to significantly enhance photocurrents. The best photovoltaic performance was obtained from the CdS/CdSe/ZnS-sensitizer with the ZnS layer on the top, yielding an overall power conversion efficiency of 3.44% with a mask around the active film and 3.90% with no mask. The effect of the mask on short-circuit current (J_{sc}) and overall efficiency (η) measurements was shown to be increasingly critical in semiconductor-sensitized solar cells as they exhibit high photocurrents. The polysulfide electrolyte, which acted as an effective electron transfer mediator for CdS and/or CdSe sensitizers, was not as effective for PbS-based sensitizers prepared by the same SILAR process.

Introduction

Recently, there has been a huge surge for finding economic and efficient carbon-free energy resources to meet future energy needs.¹ Solar energy is one of the most promising natural resources to solve the energy crisis, but current photovoltaic devices do not exhibit high enough solar-to-electric power conversion efficiencies with both cost effectiveness and necessary lifetimes.² Therefore, numerous efforts have been made to develop more efficient photovoltaic devices at lower costs. Along with new advents and progress made for last 2 decades in areas of dye-sensitized³ and bulk-heterojunction (BHJ) polymer⁴ solar cells based on organic chromophores (dyes and polymers, respectively), nanocrystalline semiconducting particles (called quantum dots, QDs) have also attracted much attention as useful building blocks in making new

types of solar cells from the inorganic light-harvesting materials.⁵ Taking advantage of nanoscale controllability and diversity in their compositions and assemblies, inorganic semiconductors (SCs) or their thin films have shown promise as the next generation sensitizers having many favorable features^{6,7} including (1) facile tunability of the effective band gaps from the visible to the IR range by simply controlling their sizes, shapes, or compositions; (2) strong absorption with high molar absorptivity; (3) high stability and resistivity toward atmospheric oxygen and water; (4) new possibilities for constructing novel structures such as multilayered- or hybrid-sensitizers; and (5) new phenomena such as multiple

*Corresponding author. E-mail: hyoje@unist.ac.kr (H.J.L.); smpark@unist.ac.kr (S.-M.P.). Phone: +82-52-217-2916. Fax: +82-52-217-2909.

- (1) (a) Barnham, K. W. J.; Mazzetti, M.; Clive, B. *Nat. Mater.* **2006**, *5*, 161. (b) Dresselhaus, M. S.; Thomas, I. L. *Nature* **2001**, *414*, 332.
- (2) (a) Atwater, H. A.; Polman, A. *Nat. Mater.* **2010**, *9*, 205. (b) Joshi, A. S.; Dincer, I.; Reddy, B. V. *Renewable Sustainable Energy Rev.* **2009**, *13*, 1884. (c) Chopra, K. L.; Paulson, P. D.; Dutta, V. *Prog. Photovoltaics: Res. Appl.* **2004**, *12*, 69.
- (3) (a) Grätzel, M. *Nature* **2001**, *414*, 338. (b) Grätzel, M. *Acc. Chem. Res.* **2009**, *42*, 1788.
- (4) (a) Peet, J.; Heeger, A. J.; Bazan, G. C. *Acc. Chem. Res.* **2009**, *42*, 1700. (b) Brabec, C. J.; Sariciftci, N. S.; Hummelen, J. C. *Adv. Funct. Mater.* **2001**, *11*, 15.

- (5) (a) Nozik, A. J. *Phys. E* **2002**, *14*, 115. (b) Huynh, W. U.; Dittmer, J. J.; Alivisatos, A. P. *Science* **2002**, *295*, 2425. (c) Luther, J. M.; Law, M.; Beard, M. C.; Song, Q.; Reese, M. O.; Ellingson, R. J.; Nozik, A. J. *Nano Lett.* **2008**, *8*, 3488. (d) Gur, I.; Fromer, N. A.; Geier, M. L.; Alivisatos, A. P. *Science* **2005**, *310*, 462.
- (6) (a) Murray, C. B.; Kagan, C. B.; Bawendi, M. G. *Annu. Rev. Mater. Sci.* **2000**, *30*, 545. (b) Sargent, E. H. *Adv. Mater.* **2008**, *20*, 3958. (c) Burda, C.; Chen, X. B.; Narayanan, R.; El-Sayed, M. A. *Chem. Rev.* **2005**, *105*, 1025. (d) Schaller, R. D.; Klimov, V. I. *Phys. Rev. Lett.* **2004**, *92*, 186601.
- (7) (a) Kamat, P. V. *J. Phys. Chem. C* **2008**, *112*, 18737. (b) Hodes, G. *J. Phys. Chem. C* **2008**, *112*, 17778. (c) Lee, Y.-L.; Lo, Y.-S. *Adv. Func. Mater.* **2009**, *19*, 604. (d) Lee, H. J.; Leventis, H. C.; Moon, S.-J.; Chen, P.; Ito, S.; Haque, S. A.; Torres, T.; Nüesch, F.; Geiger, T.; Zakeeruddin, S. M.; Grätzel, M.; Nazeeruddin, Md. K. *Adv. Funct. Mater.* **2009**, *19*, 2735. (e) Lee, H. J.; Wang, M.; Chen, P.; Gamelin, D. R.; Zakeeruddin, S. M.; Grätzel, M.; Nazeeruddin, Md. K. *Nano Lett.* **2009**, *9*, 4221. (f) Buhbut, S.; Itzhakov, S.; Tauber, E.; Shalom, M.; Hod, I.; Geiger, T.; Garini, Y.; Oron, D.; Zaban, A. *ACS Nano* **2010**, *4*, 1293.

excition generation (MEG) and energy transfer-based charge collection. However, the progress for SC-based solar cells has not been too impressive with many challenging problems left to be solved before their implementation to the construction of efficient and stable photovoltaic devices.

While QDs or their thin films, often termed as an extremely thin absorber (ETA), appeared to be one of the most promising candidates among a few different types of sensitizers in replacing typical molecular dyes in dye-sensitized solar cells (DSSCs),⁷ many of them did not fully demonstrate their favorable intrinsic properties due to poor hole carriers and the corrosive nature of many electrolyte solutions.⁸ Since many efforts have been made on finding appropriate hole conductors for the past decade since the first report on it,^{8a} investigators in this area are now in a good position to evaluate SC-sensitized photoanodes in a sandwich-type cell with regenerative redox couples such as cobalt(II/III) complex-based couples in organic solvents^{7e,9} or polysulfides (S^{2-}/S_n^{2-}) in aqueous or water-methanol mixed electrolytes.^{7c,10} It is not too difficult to find reports on SC-sensitized solar cells based on mesoporous metal oxides working in regenerative modes that show higher than 1% overall efficiencies.^{9–13} Recently, those SC-sensitized cells reached about 4% overall power conversion efficiencies using these electrolytes after optimizing many parameters.^{7c,e} In particular, multilayered semiconductor-sensitizers including CdSe QDs or their thin films with inner (CdS)- and/or outer

(ZnS)-layers have recently shown impressive results when tested with polysulfide electrolytes.^{7c,10a,b,g–i,12} The multilayered (CdS)/CdSe/(ZnS)-sensitizers have exhibited short-circuit currents comparable to those of DSSCs and are thus being considered as an important model system in semiconductor-sensitized solar cells. However, preparative routes of each layer, in which metal sulfides were prepared by a typical SILAR procedure while the main absorbing CdSe was deposited by typical chemical bath deposition (CBD)^{10a,g,i,12} or electroplating,¹³ could not be regarded as a general and unified procedure for preparing multicomponent photoanodes. It is well accepted that different methods of preparing semiconductor sensitizers would lead to solar cells of different overall properties resulting in different efficiencies. Therefore, it is highly desirable to prepare both the main absorber layer of CdSe as well as under- or overlayers made of CdS or ZnS using the all SILAR process, which boasts facile and reproducible preparation with a reasonably good controllability in growing the target materials even on mesoporous TiO₂ surfaces.¹⁴

In this study, the model sensitizer of all three SC layers, CdS/CdSe/ZnS, was prepared successively by a series of SILAR procedures in reproducible and controllable ways. The multilayered SC-sensitized solar cells thus prepared yielded high enough short-circuit currents that mask effects must now be considered as for DSSCs. We also prepared multilayered lead sulfide (PbS) SC-based sensitizers by the all SILAR process and report their photovoltaic properties in the same polysulfide electrolyte solution.

Experimental Method

- Chemicals and Materials.** Cadmium nitrate tetrahydrate (Aldrich, 98%), lead nitrate (Aldrich, 99.999%), zinc nitrate hexahydrate (Aldrich, 98%), selenium dioxide (Aldrich, 99.9+%), sodium sulfide (Aldrich), titanium diisopropoxide bis(acetyl-acetonate) (Aldrich), sulfur (Aldrich, 99.98%), potassium chloride (Acros Organics), hexachloroplatinic acid hexahydrate (Sigma-Aldrich), and sodium borohydride (Aldrich, >98.5%) were used as received. Ethanol and methanol were of HPLC grade. Titanium dioxide pastes (Ti-Nanoxide, T20/SP and R/SP) and FTO glasses (TCO30-8 and TCO22-15) for working and counter electrodes, respectively, were obtained from Solaronix.
- Growth of Multilayered Semiconductors (CdS4/CdSe7/ZnS1 and PbS5/CdS1/ZnS1) by SILAR Processes.** The optimized TiO₂/FTO film was successively immersed into two different solutions for 5 min each, first in 0.50 M Cd(NO₃)₂ in ethanol and then in 0.20 M Na₂S in methanol/water (7:3/v:v). Following each immersion, the films were rinsed for 3 min or longer with pure ethanol and methanol, respectively, to remove excess precursors and dried before the next dipping. This immersion cycle was repeated four times for the CdS layer (designated as “CdS4”). For CdSe deposition, 0.050 M Cd(NO₃)₂ and 0.050 M sodium selenide in ethanol were used for seven successive SILAR processes with a dipping time of 1 min each (“CdSe7”). Sodium selenide (Na₂Se) was prepared in situ by adding 0.1133 g of NaBH₄ (to make up 0.10 M) to 0.050 M SeO₂ in 30 mL of
- (8) (a) Zaban, A.; Micic, O. I.; Gregg, B. A.; Nozik, A. J. *Langmuir* **1998**, *14*, 3153. (b) Leschke, K. S.; Divakar, R.; Basu, J.; Enache-Pommer, E.; Boercker, J. E.; Carter, C. B.; Kortshagen, U. R.; Norris, D. J.; Aydil, E. S. *Nano Lett.* **2007**, *17*, 1793. (c) Lee, Y.-L.; Chang, C.-H. *J. Power Sources* **2008**, *185*, 584.
- (9) (a) Yu, P.; Zhu, K.; Norman, A. G.; Ferrere, S.; Frank, A. J.; Nozik, A. J. *J. Phys. Chem. B* **2006**, *110*, 25451. (b) Lee, H. J.; Yum, J.-H.; Leventis, H. C.; Zakeeruddin, S. M.; Haque, S. A.; Chen, P.; Seok, S. I.; Grätzel, M.; Nazeeruddin, Md. K. *J. Phys. Chem. C* **2008**, *112*, 11600. (c) Lee, H. J.; Chen, P.; Moon, S.-J.; Frédéric, S.; Sivula, K.; Bessho, T.; Gamelin, D. R.; Comte, P.; Zakeeruddin, S. M.; Seok, S. I.; Grätzel, M.; Nazeeruddin, Md. K. *Langmuir* **2009**, *25*, 7602.
- (10) (a) Diguna, L. J.; Shen, Q.; Kobayashi, J.; Toyoda, T. *Appl. Phys. Lett.* **2007**, *91*, 023116. (b) Lee, Y.-L.; Huang, B.-M.; Chien, H.-T. *Chem. Mater.* **2008**, *19*, 1626. (c) Chi, C.-F.; Liau, S.-Y.; Lee, Y.-L. *Nanotechnology* **2010**, *21*, 25202. (d) Fan, S.-Q.; Fang, B.; Kim, J. H.; Kim, J.-J.; Yu, J.-S.; Ko, J. *Appl. Phys. Lett.* **2010**, *96*, 63501. (e) Mora-Seró, I.; Giménez, S.; Moehl, T.; Fabregat-Santiago, F.; Lana-Villarreal, T.; Gómez, R.; Bisquert, J. *Nanotechnology* **2008**, *19*, 424007. (f) Giménez, S.; Mora-Seró, I.; Macor, L.; Guijarro, N.; Lana-Villarreal, T.; Gómez, R.; Diguna, L. J.; Shen, Q.; Toyoda, T.; Bisquert, J. *Nanotechnology* **2009**, *20*, 295204. (g) Sudhagar, P.; Jung, J. H.; Park, S.; Lee, Y.-G.; Sathyamoorthy, R.; Kang, Y. S.; Ahn, H. *Electrochim. Commun.* **2009**, *11*, 2220. (h) Fan, S.-Q.; Kim, D.; Kim, J.-J.; Jung, D. W.; Kang, S. O.; Ko, J. *Electrochim. Commun.* **2009**, *11*, 1337. (i) Shen, Q.; Kobayashi, J.; Diguna, L. J.; Toyoda, T. *J. Appl. Phys.* **2008**, *103*, 084304.
- (11) (a) Chang, C.-H.; Lee, Y.-L. *Appl. Phys. Lett.* **2007**, *91*, 053503. (b) Lin, S.-C.; Lee, Y.-L.; Chang, C.-H.; Shen, Y.-J.; Yang, Y.-M. *Appl. Phys. Lett.* **2007**, *90*, 143517. (c) Lee, W.; Lee, J.; Lee, S.; Yi, W.; Han, S.-H.; Cho, B. W. *Appl. Phys. Lett.* **2008**, *92*, 153510. (d) Laramona, G.; Choné, C.; Jacob, A.; Sakakura, D.; Delatouche, B.; Pérez, D.; Cieren, X.; Nagino, M.; Bayon, R. *Chem. Mater.* **2006**, *18*, 1688.
- (12) Niitsuu, O.; Sarkar, S. K.; Pejoux, C.; Rühle, S.; Cahen, D.; Hodges, G. *J. Photochem. Photobiol., A* **2006**, *181*, 306.
- (13) (a) Lévy-Clément, C.; Tena-Zaera, R.; Ryan, M. A.; Katty, A.; Hodges, G. *Adv. Mater.* **2005**, *17*, 1512. (b) Tena-Zaera, R.; Katty, A.; Bastide, S.; Lévy-Clément, C. *Chem. Mater.* **2007**, *19*, 1626.
- (14) (a) Pathan, H. M.; Lokhande, C. D. *Bull. Mater. Sci.* **2004**, *27*, 85. (b) Park, S.; Clark, B. L.; Keszler, D. A.; Bender, J. P.; Wager, J. F.; Reynolds, T. A.; Herman, G. S. *Science* **2002**, *297*, 65.

ethanol while the container was purged with Ar or N₂.^{7e} For ZnS capping, 0.10 M Zn(NO₃)₂ in ethanol and 0.10 M Na₂S in methanol/water (7:3/v:v) were used for a 1 SILAR process with a dipping time of 1 min each (“ZnS1”). For PbS deposition from their precursor solutions, the TiO₂ film-modified electrode was dipped into 0.020 M Pb(NO₃)₂ in methanol, rinsed with pure methanol and then dried in air, followed by the same process for uptake of the counteranion (S²⁻) from 0.020 M Na₂S in methanol for 1 min each. Such an immersion cycle was repeated five times (“PbS5”). For CdS1 and/or ZnS1 capping, exactly the same procedure as described above for depositing CdS/CdSe/ZnS was used over the PbS/TiO₂ electrode with 1 SILAR cycle each (“CdS1” and “ZnS1”).

Electrolyte Solution. The polysulfide electrolyte solution was prepared freshly prior to each measurement by dissolving 0.60 M Na₂S, 0.20 M S, and 0.20 M KCl in water/methanol (7:3/v:v).

Fabrication of Semiconductor-Sensitized Photoelectrochemical Cells. Photoelectrodes were prepared with a TiO₂ film having a double layer structure. A compact blocking underlayer of spray-pyrolyzed titanium dioxide (~150 nm thick) was deposited by spraying an ethanol solution of titanium diisopropoxide bis(acetylacetone) (0.020 M) 16 times onto a cleaned conducting glass substrate (F-doped SnO₂, resistance 8 Ω sq⁻¹), which was maintained at 450 °C. The treated glass plate was then fired at 450 °C for 30 min to remove remaining organic traces. An optimized mesoporous TiO₂ film (~12 μm thick) was prepared by doctor blade-printing of a commercial TiO₂ paste (Ti-Nanoxide, T20/SP) after it had been diluted by pure ethanol, and the sintering temperature was gradually increased up to 550 °C over 90 min and maintained for another 30 min. The TiO₂ nanocrystalline oxide films were then coated with SC sensitizers via a series of typical SILAR processes in alcoholic (or alcohol–water mixed) solutions containing each target ion. All SILAR processes were carried out at room temperature in air except for CdSe deposition; sodium selenide was kept under an inert atmosphere as it is not stable in air. It was found that the selenide generated in situ is stable for a few hours inside a glovebag after purging with nitrogen or argon. Thus, a typical SILAR process was carried out at room temperature inside a glovebag for the CdSe deposition. After rinsing the SC-modified electrode with an appropriate solvent, it was assembled into a cell using a counter electrode facing it, which had been prepared by chemical deposition of 0.050 M hexachloroplatinic acid in ethanol at 400 °C for 20 min onto an FTO glass. The cell was then sealed with a 50 μm thick transparent hot-melt film (Himilan of Mitsui-DuPont poly chemical) by hot-pressing. The electrolyte was injected into the interelectrode space from the counter electrode side through a predrilled hole, which was then sealed with a Himilan sheet and a thin glass slide cover by heating. The procedure for preparing electrodes and assembling cells was the same as that for typical DSSCs except for one step of modifying the mesoporous TiO₂ film by semiconductor layers.

Photocurrent–voltage Measurements. A class A solar simulator (model, 91195A) from Newport, which has a 450 W xenon lamp with an irradiance of 100 mW cm⁻² (equivalent to one sun at AM 1.5) at the surface of the solar cell, was used. The spectral output of the lamp was calibrated using a standard silicon solar cell (PV Measurements, Inc.). The current–voltage characteristics of the cell were then obtained by applying an external bias potential to the cell and measuring the photocurrent with a Keithley model 2636A digital source meter (Keithley). A black plastic tape having a slightly larger aperture (5.5 mm × 5.5 mm) than the photoactive region (5 mm × 5 mm) was used as a mask to avoid any inflated photocurrents induced by the area sur-

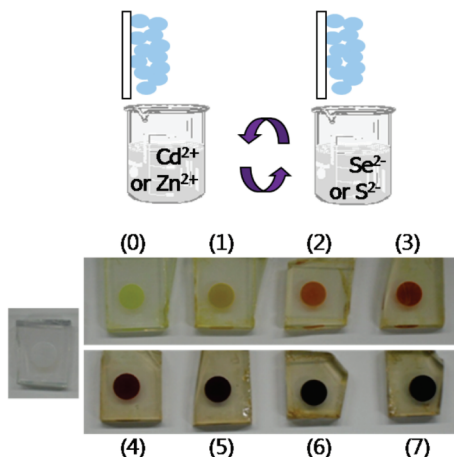


Figure 1. (Top) A simplified schematics showing a typical SILAR process for growing target semiconductor QD layers on a mesoporous TiO₂ film/FTO glass from chemical baths containing each cationic and anionic precursor. (Bottom) Pictures of resulting electrodes after each SILAR step; a bare TiO₂ film/FTO glass at the left (transparent) underwent four times of SILAR processes for CdS deposition (0), followed by each additional consecutive SILAR (1–7) process for CdSe growth.

rounding the TiO₂ film. The incident photon-to-current conversion efficiency (IPCE) was measured as a function of wavelength from 300 to 1000 nm by using a model QEX7 system (PV Measurements, Inc.).

Transmission Electron Microscopy Images and UV–Visible Spectra. High-resolution-TEM (HR-TEM) images were obtained using a JEOL JEM-2200FS instrument. The TiO₂ films with various SC sensitizers were scratched off the FTO glass and dispersed in pure ethanol, from which a few drops were taken over a TEM grid and dried for TEM images. The absorption spectra of SILAR-processed SC-laden TiO₂ films (~1.5 μm thick) were obtained by using a UV–visible spectrophotometer (S-3100, SCINCO).

Results and Discussion

SILAR Process for Preparing the CdS/CdSe/ZnS Sensitizer. Figure 1 shows a schematic diagram for the SILAR process (top) for depositing the target SC sensitizer, CdS/CdSe/ZnS, over a mesoporous TiO₂ film along with pictures taken from the electrodes thus prepared. The SILAR process has been found to be very efficient (less than a few minutes per a deposition cycle at room temperature), well controllable in size and density of the deposit (by changing experimental parameters such as the concentration of precursors and dipping times), and highly selective for growing the deposit only onto the surface of the metal oxide (not in bulk solution) in preparing the desired semiconductors upon metal oxide substrates using precursors all from solution processes.^{7e,9c,11a,d,14} The deposition and growth of CdS and CdSe films can be followed by successive color changes based on quantum confinement effects of corresponding SC growth (see the pictures of electrodes after each SILAR step in Figure 1). After four consecutive SILAR treatments by dipping the screen-printed bare TiO₂ film into Cd²⁺ and S²⁻ solutions alternately, a yellow-colored CdS-deposited TiO₂ film was obtained as expected (0). Then, the CdSe film was grown on the CdS-coated surface by the same SILAR process as was

for CdS layers. Consecutive color changes were clearly noted as the CdSe deposits get increasingly thicker during the 1–7 SILAR cycles. The electrode turned dark after six SILAR processes of CdSe deposition, indicating strong absorption of photons across the entire visible spectral range. In particular, it is worthwhile to point out that a very similar color change had been observed for growing CdSe colloids in a bulk solution using the well-known hot-injection method.^{6a} The similar behaviors shown by the two different methods manifest that the SILAR growth of CdSe QD on the metal oxide surface is as effective as the hot-injection method in the bulk solution. For now, the SILAR process offers the best method for growing the target SC layers over the substrate in a straightforward but controllable way. This simple growth of metal sulfides and/or selenides at the heterojunction can provide a valuable platform for investigation of the “light-induced charge transfer” phenomena at the interfaces and construction of useful optoelectronic devices and composite catalysts.

Absorption Spectra of SILAR-Grown (CdS)/CdSe/(ZnS) Sensitizers. After some optimization processes for the best photovoltaic performances, CdS4 and CdSe7 (the numbers indicate those of SILAR cycles) were shown to be the best choice for an underlayer and a main layer, respectively. The absorption spectra of thus prepared electrodes were recorded after each step of the SILAR; the absorbance increased with an increase in the amount of CdS and CdSe deposits on TiO₂ with the onset of the absorption gradually moving to a longer wavelength due to the decreased band gap of deposited semiconductors (Figure 2).

Generally, SILAR-deposited semiconductor layers show a monotonic increase in absorption in shorter wavelengths while the absorption edge moves to longer wavelengths.^{7e,15} This behavior was also shown by colloidal QDs prepared from the hot injection method; the QD sensitizers thus prepared show a distinct absorption peak due to a more homogeneous distribution of resulting QDs in size when compared to SILAR-grown deposits.^{6a–c} However, the broad distribution of the size of SILAR deposited SCs would not matter as long as the final SCs display a proper band position for charge transfer at the interfaces upon light absorption, and it could even be beneficial in utilizing a broad range of incident light. When a ZnS1-layer was added on the top of CdS4/CdSe7 (line 7 in Figure 2), a slight red-shift was observed only above about 600 nm due to a slight loss of the quantum confinement effect, indicating that the finally added ZnS layer hardly participates in harvesting incident light but plays roles in improving charge separation and collection at the interface between the TiO₂ and the predeposited main absorber (CdSe) as reported in recent studies.^{10a,i} The CdSe7 layer was also prepared with no CdS-underlayer (line 4 in Figure 2) and compared with CdS4/CdSe7 (line 6 in Figure 2); the electrode became darker at a faster

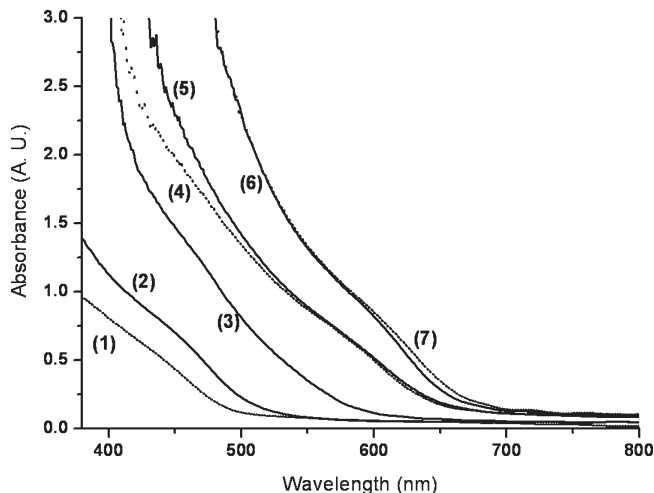


Figure 2. Absorption spectra of $\sim 1.5 \mu\text{m}$ thick films made of 20 nm TiO₂ after SILAR deposition of CdS4 (1), CdS4/CdSe1 (2), CdS4/CdSe3 (3), CdS0/CdSe7 (4), CdS4/CdSe5 (5), CdS4/CdSe7 (6), and CdS4/CdSe7/ZnS1 (7). The number after the designated semiconductors indicates repeated SILAR cycles.

rate with the CdS4 under-layer than without it. This observation indicates that the predeposited CdS layer acts as a seed for more facile CdSe growth. Thus, the CdS4/CdSe7 sensitizer (line 6) showed a higher absorption than CdSe7 (line 4) even with the contribution from the addition of CdS itself (line 1) considered.

TEM Images. It is challenging but important to directly see sensitizers on metal oxide surfaces. Reasonably clear images of SCs deposited over TiO₂ particles or nanotubes have recently been reported.^{7d,e,16} The information on the size of semiconductor particles and their distribution over the host material (TiO₂) is crucial in understanding how they are deposited as well as function at the interfaces and also in designing better deposited layers for improved sensitization. Figure 3a shows well-connected TiO₂ particles and their clean bare surfaces with an average particle size of around 20 nm as reported by the commercial source (Solaronix, Ti-Nanoxide, T20/SP). After applying the SILAR 4 times for depositing CdS, the bare surface of TiO₂ particles appears to be covered by some smaller dots (CdS) which are more clearly seen at the edge side of TiO₂ clusters (Figure 3b). The scanning TEM (STEM) image of TiO₂/CdS4 (Figure 3c) shows a clearer distribution of small CdS dots (~ 5 nm) on larger TiO₂ particles thanks to STEM’s superior capability of discriminating nanostructures of different species.¹⁷

This distribution was confirmed further by preparing CdS4 over much larger TiO₂ particles (100–200 nm from Solaronix, R/SP) in the same way to increase the contrast in size between the host (TiO₂) and guest (CdS) particles (Figure 3d). A much smaller amount of CdS was detected in the region between small dots by EDX elementary analysis when compared to the analysis right on the small dots. This observation is consistent with a previous

(15) (a) Vogel, R.; Hoyer, P.; Weller, H. *J. Phys. Chem.* **1994**, *98*, 3183.
 (b) Yang, S.-M.; Huang, C.-H.; Zhai, J.; Wang, Z.-S.; Jiang, L. *J. Mater. Chem.* **2002**, *12*, 1459.

(16) Ratanatawanate, C.; Xiong, C.; Balkus, K. J., Jr. *ACS Nano* **2008**, *2*, 1682.
 (17) http://en.wikipedia.org/wiki/Scanning_transmission_electron_microscope

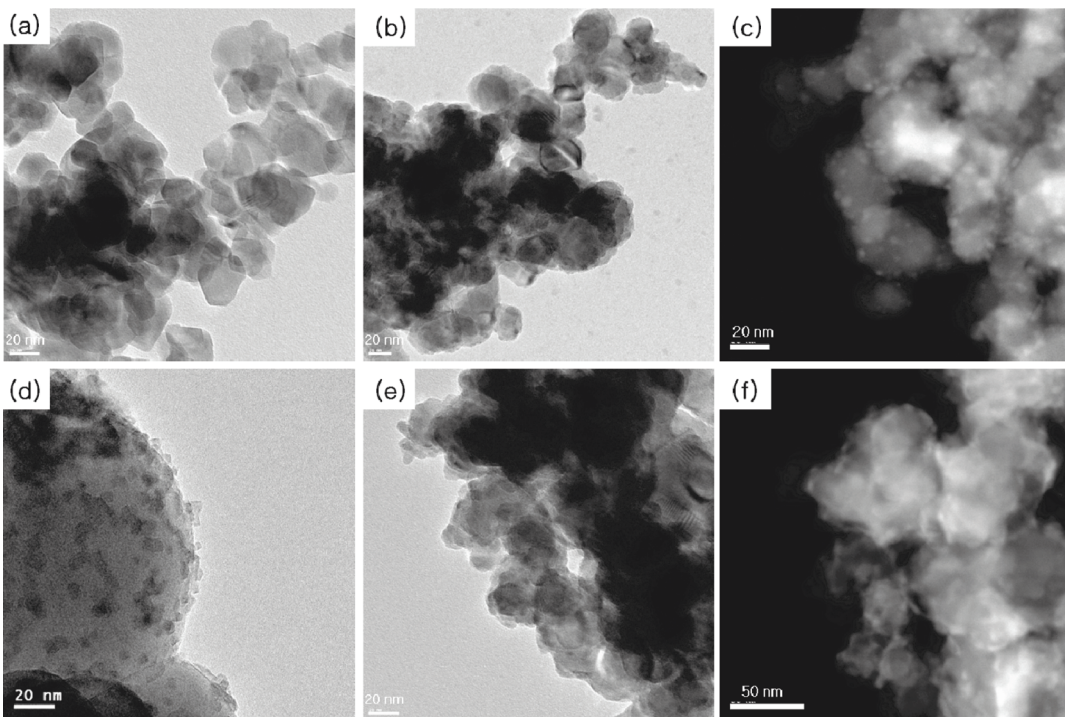


Figure 3. HR-TEM images of small pieces scraped off from (a) the bare TiO_2 film, (b) $\text{TiO}_2/\text{CdS}4$, (d) TiO_2 (100–200 nm)/ $\text{CdS}4$, and (e) $\text{TiO}_2/\text{CdS}4/\text{CdSe}7$ along with (c) scanning TEM images of $\text{TiO}_2/\text{CdS}4$ and (f) $\text{TiO}_2/\text{CdS}4/\text{CdSe}7$. All the scale bars are 20 nm long except for part f where it is 50 nm.

report,^{11d} in which small dots (CdS) were seen to be distributed on ~ 40 nm TiO_2 particles and a very thin CdS film was also reported to be present over all the TiO_2 surfaces. From the direct visual TEM images and experimental conditions used for CdS deposition, its growth mechanism and the roles as an underlayer for the main absorber, CdSe, can be inferred; Cd and S ions are delivered by the first or second SILAR cycle to directly contact the bare surface of TiO_2 , which are then used up to form a very thin conformal covering film on the bare TiO_2 surface. After this initial “wetting,” Cd and S ions delivered during the next cycles are now accumulated on the CdS thin layer. Thanks to a less-strained condition between delivered ions and substrates, CdS nucleation is accelerated and grown further to make small dots as shown in Figure 3b–d. More detailed experiments are currently in progress for a better understanding of this important process (nanocluster nucleation, growth, and coarsening at heterojunctions) during the fixation of semiconductor sensitizers on the metal oxide surface. Now with the CdS underlayer, the nucleation and growth of CdSe can be accelerated due to less-mismatched lattice constants and more similar chemistries between TiO_2/CdS and CdSe than those between TiO_2 and CdSe as observed by faster color changes and higher absorbance. Finally, many aggregated dots cover up the almost entire surface of TiO_2 particles after seven SILAR CdSe growths on $\text{TiO}_2/\text{CdS}4$, which must have grown around CdS dots and emerged into larger aggregates (Figure 3e). When a STEM image of $\text{TiO}_2/\text{CdS}/\text{CdSe}$ was obtained (Figure 3f), smaller aggregated dots (CdS/CdSe) are shown to cover the most surface of larger TiO_2 particles, thus giving a poorer contrast between CdS/CdSe and

TiO_2 than for the case of CdS and TiO_2 (Figure 3c). Putting together all the information obtained from Figures 1–3, we reach a few conclusions: (1) the CdS underlayer covers almost all the TiO_2 surface with ~ 5 nm dots distributed homogeneously; (2) the CdS underlayer promotes the growth of the upcoming CdSe layer particularly around CdS dots, leading to more CdSe accumulated on TiO_2 particles; (3) the nanoscale CdSe layer showing quantum confinement effects grows well by typical SILAR processes on TiO_2/CdS and then aggregates with each other, being affected by the presence of the CdS underlayer; and (4) the ZnS overlayer passivates the top of CdS/CdSe sensitizers without affecting the absorbance of the CdS/CdSe layer.

Mask Effects. Recently, SC-sensitized photoelectrochemical cells have been reported to show relatively high overall efficiencies (around 3–4%) based on high short-circuit currents ($> 12 \text{ mA/cm}^2$) in polysulfide electrolytes; these are comparable to those of typical DSSCs although open circuit voltages (V_{oc}) and fill factors (FF) are still not as high as those of DSSCs.^{7c,10} However, high photocurrents reported might have been overestimated due to the measurements made with no appropriate shading mask used around the active area (i.e., the SC-stained TiO_2 film) to prevent stray light from producing photocurrents as recently debated on accurate efficiencies of DSSCs in the literature.¹⁸ The differences between photocurrents

(18) (a) Ito, S.; Nazeeruddin, Md. K.; Liska, P.; Comte, P.; Charvet, R.; Pechy, P.; Jirousek, M.; Kay, A.; Zakeeruddin, S. M.; Grätzel, M. *Prog. Photovoltaics: Res. Appl.* **2006**, *14*, 589. (b) Park, J.; Koo, H.-J.; Yoo, B.; Yoo, K.; Kim, K.; Choi, W.; Park, N.-G. *Sol. Energy Mater. Sol. Cells* **2007**, *91*, 1749. (c) Lee, G.-W.; Kim, D.; Ko, M. J.; Kim, K.; Park, N.-G. *Sol. Energy* **2010**, *84*, 418.

Table 1. Short Circuit Currents, Open Circuit Voltages, Fill Factors, And Overall Conversion Efficiencies Obtained from Various Combinations of Semiconducting Sensitizers and TiO₂ Films of Different Thicknesses^a

sensitizer (thickness of TiO ₂ film)	<i>J</i> _{sc} (mA/cm ²)	<i>V</i> _{oc} (V)	FF	efficiency (%)
CdS4 (12 μm)	3.04 (3.46)	0.44 (0.46)	0.32 (0.30)	0.43 (0.48)
CdSe7 (12 μm)	7.52 (8.76)	0.48 (0.49)	0.56 (0.52)	2.02 (2.23)
CdS4/CdSe7 (12 μm)	10.92 (12.84)	0.46 (0.47)	0.57 (0.54)	2.86 (3.26)
CdSe7/ZnS1 (12 μm)	10.61 (12.36)	0.50 (0.51)	0.48 (0.45)	2.55 (2.84)
CdS4/CdSe7/ZnS1 (12 μm)	13.52 (16.24)	0.48 (0.49)	0.53 (0.49)	3.44 (3.90)
CdS4/CdSe7/ZnS1 (7.5 μm)	11.64 (13.84)	0.49 (0.50)	0.51 (0.47)	2.91 (3.25)
CdS4/CdSe7/ZnS1 (3 μm)	8.96 (10.52)	0.51 (0.52)	0.48 (0.44)	2.19 (2.41)

^aThe data were observed with masks while those in parentheses were without masks.

measured with and without a mask were not insignificant when the data reported by different laboratories was compared and evaluated. Under illumination without the mask, inflated short-circuit currents by as much as 10–20% were observed when compared to properly masked-cells. These photocurrents were found to result mainly from stray light falling onto the edge of the glass substrate, which was then guided through the glass toward the photoactive area by multiple reflections.¹⁸ Therefore, it was recommended for reliable measurements that a mask with a slightly larger aperture than the measured photoactive film should be placed over the front glass substrate.¹⁸ Our SC-cells would encounter similar problems to those observed for DSSCs due to their similar cell structures used. Our observations from the SC-sensitized solar cells with and without the mask (Table 1) showed a few consistent general trends: (1) the *V*_{oc}'s stayed almost the same for both cases, although the case without a mask was slightly higher by about 10 mV due to the higher current flowing, leading to a higher Fermi level of electrons in TiO₂; (2) fill factors were improved by about 0.02–0.04 with masks due to decreased series resistances caused by reduced currents flowing through masked cells; and (3) most importantly, the masks affected measured short-circuit currents to a large extent. Thus, the currents were overestimated by about 15–20% without masks. Overall, those changes were translated into an overestimation of the 10–14% power conversion efficiency in SC-sensitized cells. The overestimation becomes more significant as the overall efficiency increases (>3%) due to the enhanced short-circuit current. Therefore, a caution should be taken to define both the accurate area of the active layer and the precise light intensity projecting on the active layer when handling a high short circuit current solar cell constructed over glass substrates.^{18,19} Now, SC-based solar cells have entered into the stage where the “mask effect” must be considered seriously for accurate measurements and comparisons as for DSSCs.

Photovoltaic Tests. To scrutinize roles and effects of each layer in the CdS/CdSe/ZnS-sensitizer, we prepared a variety of combinations of SC layers on TiO₂ films, evaluated their photovoltaic performances in polysulfide electrolytes in regenerative sandwich-type cells, and summarized the results in Table 1. Generally, the TiO₂ photoanode with multicomponent sensitizers gave higher

short-circuit currents (>10 mA/cm²) than single-component counterparts. The single component CdSe7-sensitized cell gave about a 2% overall efficiency while the CdS4-sensitized cell exhibited a 0.43% power conversion efficiency. These results clearly indicate that the main sensitization comes from CdSe due to its wider spectral response than that of CdS. When both were combined sequentially as in CdS/CdSe, synergistic improvements in *J*_{sc} were always observed with slight changes in *V*_{oc} and FF values, leading to ~3% conversion efficiencies. The large increase in photocurrents appears to originate from not only the favorable realignment of the Fermi level at TiO₂/CdS/CdSe interfaces for facile charge flows as suggested in recent results^{7c} but also effective seeding of CdS for depositing more CdSe. The latter effect was confirmed by the absorption spectra presented in Figure 2. Both CdS and CdSe SC layers thus prepared appear to contribute to the generation of higher currents due to the favorable alignment of energy levels with polysulfide electrolytes as well. The CdS under-layer was found to be critical in enhancing the performance to over 3% by boosting the photocurrents. In addition to the CdS under-layer, the ZnS overlayer was also shown to be effective in improving the overall efficiency in recent reports.^{10i,20} A single ZnS deposition by one SILAR process led to an increase in photocurrents by as much as for the case of the CdS-under-layer with a slight increase in *V*_{oc} but a decrease in FF. A relatively thick ZnS layer can block the whole regenerative process of CdSe, but a thin passivation shell formed by 1–2 SILAR processes not only helps reduce the photoinduced excitons that can be trapped in many surface states of bare CdSe but also prevent the leakage current from CdSe to the electrolytes due to its higher conduction band. Those effects of the ZnS overlayer on the photovoltaic performance were further investigated by impedance techniques in a recent report,²⁰ which clearly showed that the ZnS coating reduced the recombination of electrons from TiO₂ with the oxidized form, S_n²⁻, in the electrolyte solution, increasing lifetimes of electrons in SC-sensitized cells. From the multicomponent CdS4/CdSe7/ZnS1-sensitizer, we obtained the highest *J*_{sc} of ~14 mA/cm² (with no mask, ~16 mA/cm²) in a reproducible way, leading to the best overall efficiency of ~3.5% (~3.9% without a mask) under a standard one sun condition. The best performance of this sensitizer

(19) Cravino, A.; Schilinsky, P.; Brabec, C. J. *Adv. Funct. Mater.* **2007**, 17, 3906.

(20) Mora-Seró, I.; Giménez, S.; Fabregat-Santiago, F.; Gómez, R.; Shen, Q.; Toyoda, T.; Bisquert, J. *Acc. Chem. Res.* **2009**, 42, 1848.

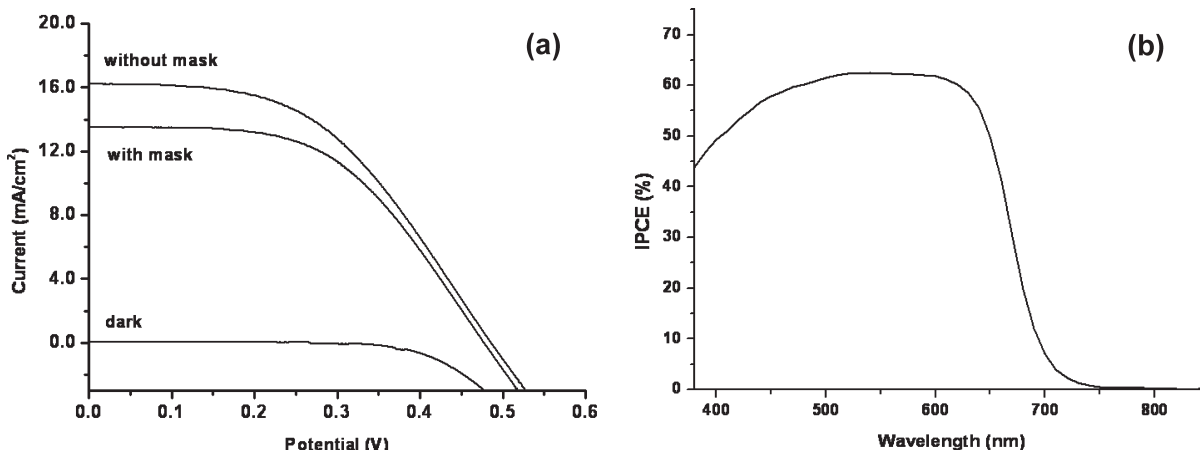


Figure 4. (a) $J-V$ curves and (b) IPCE data for the best CdS4/CdSe7/ZnS1-sensitized cell obtained in this study.

observed here is in agreement with the recently reported result^{7c} with a comparable J_{sc} value to that of DSSCs. We thus investigated more into this multilayer-structured sensitizer as a model system to understand the mechanism of its operation; we consider the CdS/CdSe/ZnS-sensitizer as a standard in SC-sensitized solar cells in the current stage just as the N719 dye in DSSCs.

Figure 4 shows current density–voltage ($J-V$) and incident photon-to-current conversion efficiency (IPCE) data for the best sensitizer when tested with a polysulfide redox couple. With comparison of the two curves from the best cell with and without mask, it is clearly shown how the mask affects the final results as already explained (Figure 4a). The cell exhibits about 60% of the incident photon-to-current conversion efficiencies over a broad range of wavelengths up to 620 nm with an onset wavelength of about 750 nm (Figure 4b). The overall conversion efficiency of ~3.5% (3.9% without mask) is one of the best records among reported CdSe-sensitized cells with a counter electrode easily prepared using a catalytic amount of platinum on FTO glass. Moreover, the observed low FF value (~0.5) might be improved further by changing the Pt catalyst to gold or Cu₂S, which were known to display a better catalytic activity for S_n²⁻ reduction.^{10f,20,21} Such studies are currently underway for finding the best performing counter electrode in the polysulfide electrolyte. It is also clearly seen from this study and recently reported data²⁰ that the FF is also heavily dependent on preparative routes of the main absorber, CdSe; our SILAR-processed CdSe-sensitized cell displayed a FF of around 0.5 while the chemical bath-deposited (CBD) CdSe-sensitized one showed about 0.3 with the same Pt-catalyzed counter electrode.²⁰ The reason for this large difference could be ascribed to different growth patterns of CdSe over TiO₂ in two cases; the SILAR-processed CdSe layers appear to grow in a more conformal way along the surface of mesoporous TiO₂ films, thus reducing direct contact areas between the bare TiO₂ surface and polysulfide electrolytes resulting in increases in shunt resistances at TiO₂/CdSe/S_n²⁻

interfaces for a higher FF of the cell. This behavior also supports that the SILAR process is more appropriate for preparing efficient CdSe sensitizers over mesoporous TiO₂ films than a typical CBD method reported thus far.^{12,20}

Effects of the TiO₂ mesoporous film thickness on the cell performance was studied by increasing the film thickness from 3 to 12 μm with the same CdS/CdSe/ZnS sensitizer. The photocurrents gradually increased with an increase in the film thickness to around 12 μm , at which the best overall efficiency was obtained (Table 1). Homogeneous deposition of the target SC layer throughout the TiO₂ film would ensure the relatively thicker film to work better than the thinner ones. However, it becomes increasingly difficult to grow a homogeneous conformal-layer of the SC sensitizers on the TiO₂ surface through narrow mesopores (< 30 nm) as the TiO₂ film becomes thicker, thus reaching an optimum point at 12 μm under our experimental conditions. With the polysulfide redox couple, the diffusion-limited behavior was not observed for photocurrents for up to a TiO₂ film thickness of ~12 μm . This guarantees that relatively thick TiO₂ films could be used without any diffusion-related problems from polysulfide ions for generating large enough currents within the SC-sensitized TiO₂ film used.

SILAR-Grown PbS/CdS/ZnS Sensitizer. Lead sulfide (PbS)-based sensitizers have also attracted much attention due to their strong absorption in the near IR region.^{6b,7d,22} However, there are only a few reports on PbS based photoelectrochemical cells.^{9c,15} In fact, it was more difficult to find a proper redox couple for the PbS sensitizer because of its small band gap and high instability toward corrosive electrolytes. To examine whether the polysulfide electrolyte is also successfully applicable to PbS-based sensitizers, PbS layers or those capped with CdS and/or ZnS, were prepared on TiO₂ mesoporous films by the same SILAR processes and their photovoltaic performances were evaluated in the polysulfide electrolyte as well. However, as summarized in Table 2,

(21) Hodes, G.; Manassen, J.; Cahen, D. *J. Electrochem. Soc.* **1980**, *127*, 544.

(22) (a) Debnath, R.; Tang, J.; Barkhouse, D. A.; Wang, X.; Pattantyus-Abraham, A. G.; Brzozowski, L.; Levina, L.; Sargent, E. H. *J. Am. Chem. Soc.* **2010**, *132*, 5952. (b) Sargent, E. H. *Nat. Photon.* **2009**, *3*, 325.

Table 2. Summarized Data Set of Short Circuit Currents, Open Circuit Voltages, Fill Factors, and Overall Conversion Efficiencies from a Various Combination of Semiconducting Sensitizers Prepared by the All SILAR Process^a

sensitizer	J_{sc} (mA/cm ²)	V_{oc} (V)	FF	efficiency (%)
PbS5	0.76	0.20	0.16	0.02
PbS5/CdS1	0.79	0.20	0.18	0.03
PbS5/ZnS1	0.63	0.20	0.17	0.02
PbS5/CdS1/ZnS1	1.50	0.32	0.20	0.10

^aThe number after designated semiconductors indicates the repeated times of each SILAR process.

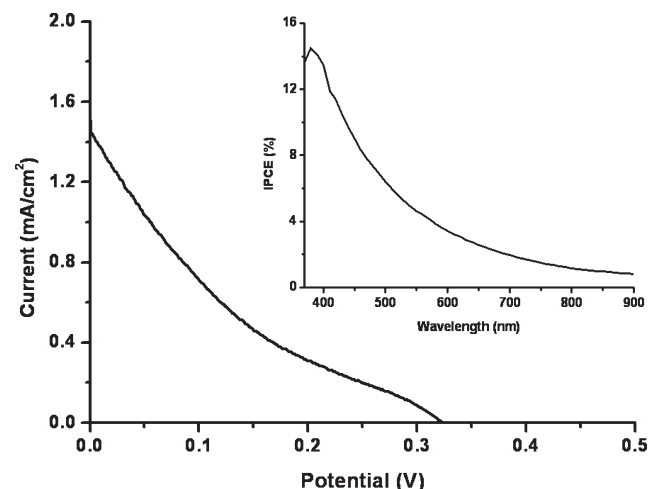


Figure 5. $J-V$ curve along with IPCE data (inset) for the best PbS5/CdS1/ZnS1-sensitized cell obtained in this study.

PbS-based sensitizers exhibited very poor performances when the polysulfide was used as a hole carrier. The single CdS or ZnS overlayer on TiO₂/PbS was not effective at all while the double overlayers (CdS/ZnS) suggested in a previous report^{15b} exhibited a positive effect on J_{sc} and V_{oc} albeit low. Figure 5 shows the best $J-V$ curve and IPCE data for the PbS5/CdS1/ZnS1 layers. Although the photovoltaic response signal was detected up to about 900 nm, the conversion efficiency was very low in a wide wavelength region (inset of Figure 5) and the $J-V$ curve shows a poor FF (0.2) along with very low J_{sc} and V_{oc} values. The main reason for these poor performances is ascribed to intrinsic properties of PbS toward the oxidized form, S_n²⁻, of the polysulfide electrolyte; PbS was reported to show a catalytic reactivity for reducing S_n²⁻,²¹ which indicates that electrons photogenerated in PbS can be transferred easily to S_n²⁻. This reverse electron flow at the PbS/S_n²⁻ interface explains why the PbS-based sensitizers showed very low J_{sc} and FF values when the polysulfide is used as a redox mediator. Another possible reason could be due to a high rate of recombination of the electrons injected into TiO₂ with the oxidized form (S_n²⁻) of the redox couple. In fact, TEM images indicated that PbS SCs were shown to be well-separated from each other under current deposition conditions.^{7d} The incomplete coverage by PbS layers over TiO₂ surface could provide many pathways of recombination, leading to the very low J_{sc} and V_{oc} values.

Conclusions

In this study, we have shown that multilayered semiconductor (CdS/CdSe/ZnS) layers were prepared on the surface of TiO₂ mesoporous films as an important model sensitizer employing a series of SILAR processes, which allow each semiconducting layer to grow successively in a reproducible and controllable manner. Addition of under- and/or overlayers to the main absorbing-semiconductor layer is a general strategy for enhancing favorable charge separation at the main absorbing layer, increasing the overall conversion efficiency by controlling and/or modifying the surface states that are very critical to determine the fate of excitons generated inside the semiconductor dots. Thus, the SILAR process offers a very promising strategy for preparing property-modulated multilayered sensitizers on the substrate by growing desired SC layers as demonstrated in this study. Along with the multilayered CdS/CdSe/ZnS sensitizers, the polysulfide electrolyte (S²⁻/S_n²⁻) was also essential in making a relatively high efficiency SC-sensitized photoelectrochemical cell. The S²⁻/S_n²⁻ redox couple has outperformed all the other candidates in photocurrent generation from chalcogenide-sensitized cells and has also shown a comparable capability for the first time for carrying charges to I⁻/I₃⁻ in DSSCs, with its currents large enough to raise an issue on the “mask effect” in SC-sensitized cells.

On the basis of our results and others reported recently,^{7c,e,22,23} it is certain that nanoscale semiconducting QDs or films having a proper band gap have proved themselves as a promising photocurrent-generator for the next generation solar cells. To further improve photovoltaic performances, it is necessary to pay more attention to hole conductors and interfacial engineering which could yield higher V_{oc} and FF values when used with semiconductor-sensitizers. Judging from the best parameters reported so far, J_{sc} (~14 mA/cm²) from our present results and V_{oc} (0.6 V) and FF (0.78) from ref 7e, in which a cobalt redox couple [Co(o-phen)₃^{2+/3+}] was used as a redox mediator, we may conclude that an overall conversion efficiency of ~6.5% would be attainable with some room for further improvement. This simple estimation based on our and reported data provides a good reason for a need to find a new redox couple with characteristics of both the polysulfide electrolyte, which is capable of efficient charge generation and transporting them without diffusion limitation, and the cobalt (II/III) complex-based redox pair, which offers a relatively high V_{oc} as well as FF with stability.

Acknowledgment. This work was supported by the World Class University program funded by the Korea Research Foundation (Grant R31-2008-000-20012-0). S. Kim thanks support by the Korea Science and Engineering Foundation (KOSEF) grant funded by the Korea government (MOST) (Grant M10703001036-08M0300-03610).

(23) Moon, S.-J.; Itzhaik, Y.; Yum, J.-H.; Zakeeruddin, S. M.; Hodes, G.; Grätzel, M. *J. Phys. Chem. Lett.* **2010**, *1*, 1524.